Journal of the Nigerian Association of Mathematical Physics,
***Volume 8* (*November 2004*).**

Numerical simulation of hole injection in high barrier metal-semiconductor short diodes

M. G. Zebaze Kana[1], R. K. Odunaike and **A. A. Oberafo**
Physics Advanced Laboratory, Sheda Science and Technology Complex, Garki, Abuja.

Abstract

A numerical investigation is carried out on effects of minority carriers on the transport parameters of one-dimensional metal-semiconductor short diodes under highly injecting conditions. The results show that at a donor concentration $N_d=10^{14}$ cm^{-3} and total current density J=0.1 μAcm^{-2}, the hole injection ratio, γ_h , decreases rapidly by a factor of more than 80% within 2μm semiconductor layer from the interface. Furthermore, a comparison of the two-carrier model adopted in this work with the Schottky model reveals a discrepancy of 30% in the lnJ-V characteristics of a diode of 0.92 eV barrier height.

pp 69 - 74

1.0 Introduction

Various workers have shown interest in metal-semiconductor devices modelling [1-10]. The mathematical model for such devices is derived from the Boltzmann transport equation and some electromagnetic consideration, given by Maxwell's equations. However due to the complexity of equations describing such junctions, the common tendency is to consider mainly the majority carrier in the transport equations, overlooking therefore the effect of minority carrier. The behaviour of a metal-semiconductor device is closely related to the distribution of carriers (electrons and holes) at the junction, and their responses to an external signal. The minority carrier injection ratio, which is the ratio of the minority current to the total current, could reach appreciable levels under certain conditions such as large barrier height, high bulk semiconductor resistivity and large forward bias. In order to quantify the contribution of these minority carriers in the transport parameters of junctions, there is therefore a need to solve numerically the steady-state metal-semiconductor device equations without simplifying assumptions.

2.0 Theory

The two-carrier model for metal-semiconductor junctions adopted in this work is an extension of the Schottky model, which takes into account the minority carrier and the semiconductor bulk region. The basic equations for this model are derived from the current transport, the Poisson's equation, and the continuity equations, which combine with carrier recombination and generation processes to give (see for example Ref. [11]):

$$\frac{dj_p}{dx} = \frac{-qn_i\,[exp\,(\frac{\bar{\mu}_n - \bar{\mu}_p}{KT}) - 1]}{\tau_{po}\,[exp(\frac{\bar{\mu}_n - E_i}{KT}) + \frac{n_1}{n_i}] + \tau_{no}\,[exp(\frac{E_i - \bar{\mu}_p}{KT}) + \frac{p_1}{n_i}]} \tag{2.1}$$

$$\frac{dE_i}{dx} = qE \tag{2.2}$$

$$\frac{d\mathrm{E}}{dx} = \frac{q}{\varepsilon}[\,n_i\,exp(\frac{E_i - \bar{\mu}_p}{KT}) - n_i\,exp(\frac{\bar{\mu}_n - E_i}{KT}) + N_d\,] \tag{2.3}$$

$$\frac{d(\bar{\mu}_n - E_i)}{dx} = \frac{j - j_p}{\mu_n n_i}exp(\frac{E_i - \bar{\mu}_n}{KT}) - q\mathrm{E} \tag{2.4}$$

$$\frac{d(\bar{\mu}_p - E_i)}{dx} = \frac{j_p}{\mu_n n_i}exp(\frac{\bar{\mu}_p - E_i}{KT}) - q\mathrm{E} \tag{2.5}$$

*Corresponding author.

where ($\bar{\mu}_n$ and $\bar{\mu}_p$) are the electrochemical potentials for electron and hole respectively, (τ_n and τ_p) are the electron and hole lifetimes respectively, q is the electronic charge, (j and j_p) represent the total current density

and the hole current density respectively, E represents the electric field, n_i is the intrinsic free electron density, N_d is the impurity donor concentration, E_i is the intrinsic level, K is the Boltzmann constant and T, the absolute temperature. Equations 1-5 constitute the five first-order differential equations describing the two-carrier model of a metal-semiconductor junction diode.

The device prototype is illustrated in Figure 1. We assume a voltage-controlled ohmic contact with no voltage drop across it. The boundary conditions for the electrochemical potentials are therefore given by

$$\bar{\mu}_n(o) = \bar{\mu}_p(o) = E_F(0) \quad (2.6)$$

$$\bar{\mu}_n(L) = \bar{\mu}_p(L) = E_F(L) \quad (2.7)$$

and

$$E_F(L) = E_F(0) + qV \ . \quad (2.8)$$

Intrinsic levels at the two contacts are related by

$$E_i(L) = E_i(0) - \phi_d + qV \ . \quad (2.9)$$

For convenience, we define

$$\phi_i = E_F(L) - E_i(L) . \quad (2.10)$$

From Equations (2. 6-2.10), we derive the five boundary conditions below:

$$\bar{\mu}_n(0) - E_i(0) = \phi_i - \phi_d \quad (2.11)$$

$$\bar{\mu}_p(0) - E_i(0) = \phi_i - \phi_d \quad (2.12)$$

$$\bar{\mu}_n(L) - E_i(L) = \phi_i \quad (2.13)$$

$$\bar{\mu}_p(L) - E_i(L) = \phi_i \quad (2.14)$$

$$E_i(0) - E_i(L) = \phi_d - qV \quad (2.15)$$

3.0 Solution Algorithm

In order to implement an efficient algorithm, there is a need to scale the above equations. To achieve that, the following change of variables is made:

$$\chi_1 = q\frac{\phi_n - \phi_n(L) - \psi + \psi(L)}{KT} \quad (3.1)$$

$$\chi_2 = q\frac{\psi - \psi(L)}{KT} \quad (3.2)$$

$$\chi_3 = -q\frac{\mathrm{E}L_E}{KT} + \frac{jL_E}{N_d\mu_{no}KT} \quad (3.3$$

$$\chi_4 = q\frac{\phi_p - \phi_p(L) - \psi + \psi(L)}{KT} \quad (3.4)$$

$$\chi_5 = -\frac{j_pL_E}{N_d\mu_{no}KT} \quad (3.5)$$

$$t = \frac{L - x}{L_E} \quad (3.6)$$

where

$$L_E = \sqrt{\frac{\mathrm{E}KT}{q^2N_d}} \quad (3.7)$$

ϕ_n and ϕ_p are the quasi-Fermi levels for electrons and holes respectively and defined as

$$\phi_n = \psi - \frac{KT}{q}ln\left(\frac{n}{n_i}\right) \quad (3.8)$$

$$\phi_p = \psi + \frac{KT}{q}ln\left(\frac{p}{n_i}\right) \quad (3.9)$$

where ψ is the electrical potential.

The new system of equations can now be written

$$\frac{d\chi_1}{dt} = \chi_3 + J - (J - \chi_5)exp(\chi_1 - \theta_n + \lambda_n) \tag{3.10}$$

$$\frac{d\chi_2}{dt} = -\chi_3 - J \tag{3.11}$$

$$\frac{d\chi_3}{dt} = 1 - exp(\theta_n - \chi_1) + exp(\chi_4 - \theta_p) \tag{3.12}$$

$$\frac{d\chi_4}{dt} = \chi_3 + J - \chi_5\, exp(\theta_p - \lambda_p - \chi_4) \tag{3.13}$$

$$\frac{d\chi_5}{dt} = \frac{-qn_i^2 L_E^2 [exp(\chi_4 - \chi_1) - 1] / N_d \mu_{no} KT}{\tau_{po}[n_i\, exp(\theta_i - \chi_1) + n_1] + \tau_{no}[n_i\, exp(\chi_4 - \theta_i) + p_1]} \tag{3.14}$$

where

$$\begin{aligned} J &= -jL_E / N_d \mu_{no} KT \\ \theta_i &= \phi_i / KT \\ \theta_n &= \theta_i - ln(N_d / n_i) \\ \theta_p &= \theta_i + ln(N_d / n_i) \\ \lambda_n &= ln(\mu_{no} / \mu_n) \\ \lambda_p &= ln(\mu_{no} / \mu_p) \end{aligned} \quad , \tag{3.15}$$

and subject to the Dirichlet boundary conditions,

$$\begin{aligned} \chi_1 &= \chi_2 = \chi_3 = 0 \;\; at \;\; t = 0 \\ \chi_1 &= \chi_4 = \frac{q\phi}{KT} \;\; at \;\; t = L / L_E \end{aligned} \tag{3.16}$$

The conventional approach to the numerical solution to the semiconductor device equations is based on the application of Newton's method to simultaneous discretized equations. However this approach has a number of limitations such as the local convergence and requires a lot of computer resources since it involves the manipulation of huge matrices for fine meshes [9]. Our algorithm solves the two-point boundary-value problem with two unknowns (u_1 and u_2), by convergent sequence of solutions of the associated two-point boundary-value problem with one unknown. The solution of the problem corresponds to finding the roots of the system

$$d_1(u_1,u_2) = 0 \tag{3.17}$$

$$d_2(u_1,u_2) = 0 \tag{3.18}$$

where $d(d_1,d_2)$ represents the deviation from the two terminal boundary conditions at t_b.

The algorithm uses a graphical approach by mapping the solution in u_1-u_2 plane. Equations (3.17) and (3.18) define two curves $\boldsymbol{C_1}$ and $\boldsymbol{C_2}$ in u_1-u_2 plane and the root of the equation, $d(u_1,u_2) = 0$ is at the intersection of the curves $\boldsymbol{C_1}$ and $\boldsymbol{C_2}$ in u_1-u_2 plane. For any choice of u_2, $d_1 = d_1(u_1)$, and can be solved in u_1. The values of u_1 and u_2 define a point of the curve $\boldsymbol{C_1}$ in u_1-u_2 plane and a value of $d_2(u_1,u_2)$ is associated to it. The solution of the system will therefore be at the point on $\boldsymbol{C_1}$ where $d_2 = 0$. Inverse interpolation is used to find the value of u_2 along $\boldsymbol{C_1}$, which zeroes d_2. The flow diagram is shown in Figure 2.

4.0 Results And Discussion

Figure 3 shows that the minority carrier injection ratio γ_h is almost constant with the distance in the vicinity of the metal, and is high for large values of the barrier height ϕ_b (*60%* of holes from $x=0$ up to $0.5\ \mu m$ for a diode of $\phi_b=0.92$ eV). γ_h decreases with the distance and is uniform beyond the depletion width. In the semiconductor neutral region, γ_h, more than 10% of holes injected for a diode with, at a donor density $N_d=10^{14}$ cm^{-3}, value significant enough to affect the current transport characteristics of the diodes even at moderate currents. The large minority carrier injection ratio observed with ϕ_b=0.92 eV is in good agreement with the prediction of Scharfetter (1965), who argued that, when the diffusion component of the current can be neglected, the hole injection ratio could be expressed as

$$\gamma_h = \frac{n_i^2}{N_d^2}\frac{\mu_p}{\mu_n}\frac{j}{j_s}, \qquad (4.1)$$

and since the saturation current, J_s, decreases exponentially with ϕ_b, γ_h becomes therefore non-negligible for high barriers, even at moderate currents. The current-voltage characteristics of diode of barrier height 0.92 eV is presented in Figure 4; it exhibits a linear portion in *InJ - V* plots. A comparative study with the one-carrier Schottky model reveals a discrepancy between the two models (30% for ϕ_B = 92eV). The current density of the Schottky model being given by

$$J = A^{**}T^2 \, exp\left(-\frac{q\phi_b}{KT}\right)\left[exp\left(\frac{qV}{KT}\right)-1\right] \qquad (4.2)$$

where the Richardson constant A^{**} is assumed to be $115\ cm^{-2}K^{-2}$ at the donor concentration $N_d = 10^{14}$ cm^3 and for a diode $10\mu m$ thick. The large deviation observed is caused by the high hole injection, occurring in diodes of high barrier heights. Tove *et al* (1983) argued that the accuracy of Schottky barrier height determination from I-V and C-V data is worse for high barriers and low doping. The discrepancy was suspected to be caused by the large hole injection occurring at high barriers and low doping levels.

5.0 Conclusion

In this work, an accurate iterative algorithm for solving the two-carrier model of metal-semiconductor diodes is described. The results obtained show clearly that the hole injection ratio could be as high as 10% in the semiconductor neutral region of a metal-semiconductor diode and consequently the minority carriers in such cases unlike in Schottky should be taken into account in the current transport parameters of the device. Furthermore a deviation of up to 30% in *lnJ-V* plot is recorded between the two-carrier model and the Schottky model.

Acknowledgement

The authors are grateful to the Director-General of Sheda Science & Technology Complex (SHESTCO) for providing facilities for this research work. Similar thank goes to the technical personnel in the Physics Advanced Laboratory, SHESTCO, for their cooperation.

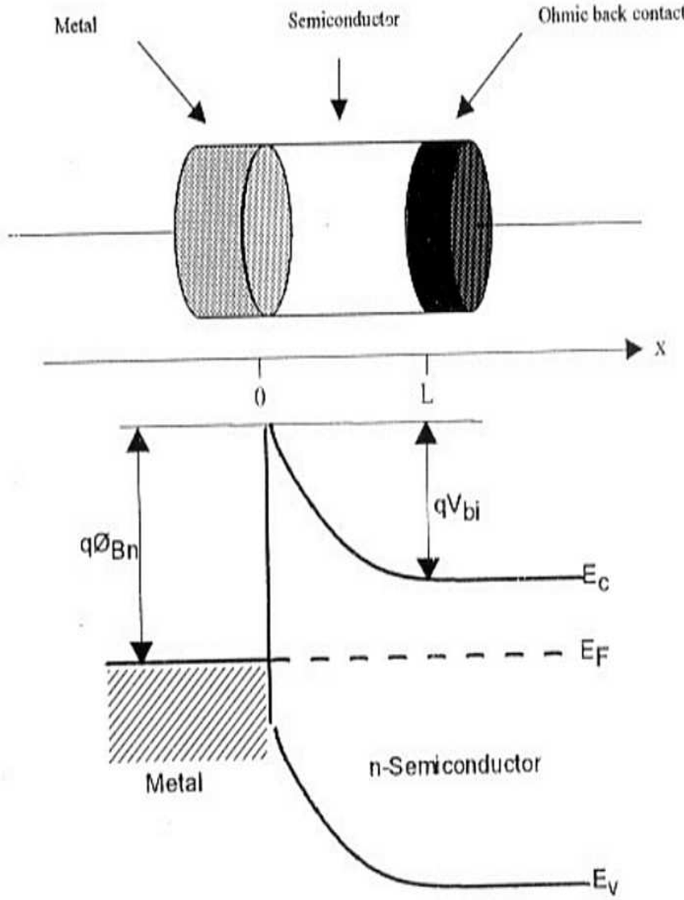

Figure 1 Device Prototype

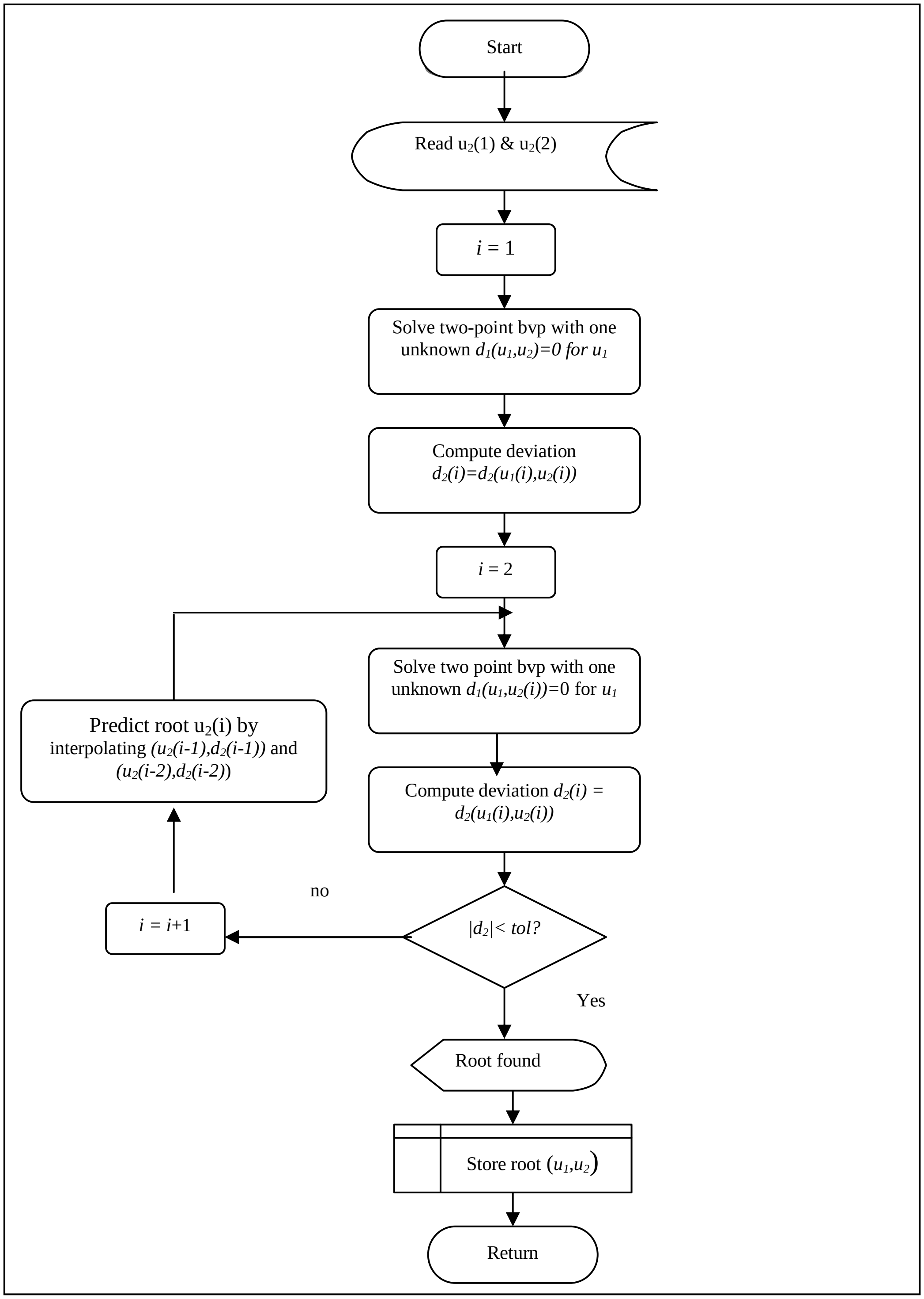

Figure 2: Flow diagram

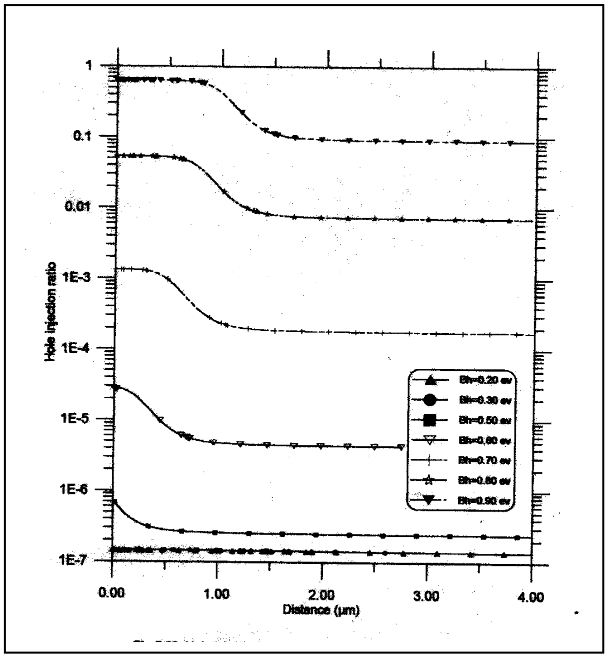

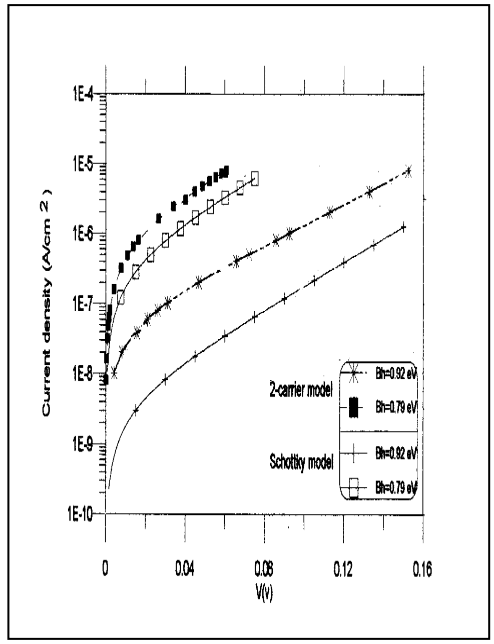

Figure 4: ln J –V plots for the two-carrier model and the Schottky model at different barrier heights

Figure 3: Variation of the hole injection ratio with the distance at various barrier heights

References

[1] Shockley, W., The Theory of p-n Junction in Semiconductors and p-n Junction Transistors, *Bell Syst. Techn. J.* 28: 435-445 (1949).

[2] Gummel, H. K., A Self-Consistent iterative Scheme for one-Dimensional Steady State Transistor Calculations, *IEEE Trans*., ED-20, 455-465 (1964).

[3] De Mari, A., An Accurate Numerical Steady-State One-Dimensional Solution of the p-n Junction. *Solid-St. Electron.* 11(1), 33-58 (1968).

[4] Scharfetter, D. L., and Gummel, H. K., Large-Signal Analysis of a Silicon Read Diode Oscillator, *IEEE Trans*., ED-16, 64-67 (1969).

[5] Alam M. A. and Lundstrom M.S., Simulation of Compound Semiconductor Devices using a Scattering Matrix Approach, Semicond. Sci. Technol. 9, 862-864 (1984).

[6] McAndrew C.C., Heasell E.L. and Singhal K., A Comprehensive Transport Model for Semiconductor Devices Simulation, Semicond. Sci. Technol. 2, 643-648 (1987).

[7] Chang K.M., A Consistent Model for Carrier Transport in Heavily Doped Semiconductor Devices, Semicond. Sci. Technol. 3, 766-772 (1988).

[8] Deng H. and Steeds J.W., Theoretical Studies of Minority Carrier Concentration Profile and Cathodoluminescence intensity in Thin-Film Materials with Different Surface Recombination Velocities aand Constant Excitation Density, Semicond. Sci. Technol. 7, 125-134 (1992).

[9] Micheletti, S., Quarteroni, A., and Sacco, R., Current-Voltage Characteristics Simulation of Semiconductor Devices using Domain Decomposition. *J. Comput. Phys*. 119: 46-61 (1995).

[10] Miller J.J.H., Schilders W.H.A. and Wang S., Application of Finite ElMethods to the Simulation of semiconductor Devices, Rep. Prog. Phys. 62, 277-353 (1999).

[11] Zebaze Kana M.G., and Oberafo, A.A., (2003); Submitted to Materials Sci. Journal

[12] Scharfetter, D. L., Minority Carrier Injection and Charge Storage in Epitaxial Schottky Barrier Diodes, Solid-St. Electron. 8: 299-311 (1965).

[13] Tove, P. A., Bohlin, K., and Norde, H., Computer Modelling of High Barrier Schottky Diodes Applied to Study of Accuracy of Experimental Barrier Determination. *Surface Science* 132: 264-257 (1983).